Supplementary Information (SI) for Nanoscale.
This journal is © The Royal Society of Chemistry 2026

Electronic Supplementary Information

Aggregation-Induced Emissive Copper(I) Clusters: From Photophysical Mechanisms to Photocatalytic Performance

Ya-Na Yu[a], Minjian Wu[a], Linhua Wang[a], Zihao Jiang[a], Jing Wang[a], Fei Xu[a], Lin Qin*[b], Liao-Yuan Yao*[a], Guo-Yu Yang*[a]

a. *MOE Key Laboratory of Cluster Science, Beijing Key Laboratory of Photoelectric/ Electrophotonic Conversion Materials, School of Chemistry and Chemical Engineering, Beijing Institute of Technology, Beijing 102488, P. R. China. E-mail: lyyao@bit.edu.cn, ygy@bit.edu.cn.*

b. *Key Laboratory of Agro product Quality and Safety, Institute of Vegetables and Flowers, Chinese Academy of Agricultural Sciences, Beijing 100081, China; E-mail: qinlin01@caas.cn.*

Table S1. Crystal data for **Cu_3**

Empirical formula	$C_{93}H_{74}Cu_3O_4P_6$
Formula weight	1631.96
Temperature/K	100.00(10)
Crystal system	hexagonal
Space group	$P6_5$
a/Å	24.2269(6)
b/Å	24.2269(6)
c/Å	28.2438(7)
α/°	90
β/°	90
γ/°	120
Volume/Å^3	14356.5(8)
Z	6
ρ_{calcg}/cm^3	1.133
μ/mm^{-1}	0.804
F(000)	5046.0
Radiation	Mo Kα (λ = 0.71073)
2Θ range for data collection/°	4.43 to 61.918
Index ranges	$-26 \le h \le 33$, $-34 \le k \le 19$, $-28 \le l \le 39$
Reflections collected	73567
Independent reflections	22507 [R_{int} = 0.0845, R_{sigma} = 0.1171]
Data/restraints/parameters	22507/698/878
Goodness-of-fit on F^2	1.042
Final R indexes [I>=2σ (I)]	R_1 = 0.0908, wR_2 = 0.2427
Final R indexes [all data]	R_1 = 0.1324, wR_2 = 0.2715
Largest diff. peak/hole / e Å^{-3}	1.36/-1.08
Flack parameter	-0.01(2)

Table S2. Bond Lengths for **Cu$_3$**

Cu01-Cu02	2.5825(14)	C18-C020	1.3900
Cu01-Cu03	2.5761(14)	C020-C02E	1.422(15)
Cu01-P004	2.280(2)	C00V-C011	1.385(17)
Cu01-P005	2.289(2)	C00X-C01D	1.400(15)
Cu01-C00A	2.098(9)	C00X-C01W	1.362(16)
Cu01-C017	2.197(10)	C00Z-C018	1.377(14)
Cu02-Cu03	2.5875(19)	C010-C01B	1.401(19)
Cu02-P006	2.272(2)	C010-C01O	1.43(2)
Cu02-P007	2.279(3)	C012-C016	1.371(15)
Cu02-C00A	2.248(10)	C014-C01A	1.34(2)
Cu02-C017	2.127(10)	C014-C01W	1.34(2)
Cu03-P008	2.263(3)	C015-C016	1.362(17)
Cu03-P009	2.273(3)	C015-C01U	1.37(2)
Cu03-C00A	2.102(9)	C017-C02E	1.197(17)
Cu03-C017	2.219(15)	C01B-C01Q	1.431(17)
P004-C00C	1.841(10)	C01C-C01K	1.40(2)
P004-C00L	1.817(8)	C01F-C01H	1.42(3)
P004-C00S	1.849(9)	C01F-C01M	1.34(2)
P005-C00E	1.827(11)	C01G-C01M	1.451(17)
P005-C00J	1.824(9)	C01G-C01V	1.27(3)
P005-C00Q	1.850(8)	C01H-C026	1.38(2)
P006-C00M	1.831(10)	C01I-C01Z	1.376(19)
P006-C019	1.814(12)	C01K-C01Z	1.41(2)
P006-C01L	1.842(7)	C01O-C02A	1.33(2)
P007-C00S	1.833(8)	C01Q-C023	1.28(2)
P007-C010	1.829(11)	C01U-C01X	1.43(2)
P007-C012	1.795(12)	C01V-C026	1.38(3)
P008-C00Q	1.818(10)	C022-C021	1.3900
P008-C01M	1.827(18)	C022-C025	1.3900
P008-C01R	1.755(7)	C021-C02H	1.3900
P009-C019	1.843(8)	C02H-C02K	1.3900
P009-C021	1.767(8)	C02K-C027	1.3900
P009-C01T	2.059(9)	C027-C025	1.3900
C00A-C00K	1.211(14)	C023-C02A	1.53(3)
C00B-C00E	1.428(14)	C024-C013	1.3900
C00B-C011	1.379(17)	C024-C8	1.3900
C00C-C00P	1.353(15)	C013-C01L	1.3900
C00C-C01I	1.375(13)	C01L-C13	1.3900
C00D-C00F	1.359(13)	C13-C11	1.3900
C00D-C00J	1.409(13)	C11-C8	1.3900
C00E-C00G	1.392(13)	C028-C01J	1.3900
C00F-C00I	1.361(15)	C028-C01N	1.3900
C00G-C00H	1.366(16)	C01J-C02G	1.3900

C00H-C00V	1.412(16)	C02G-C02C	1.3900
C00I-C018	1.375(14)	C02C-C01R	1.3900
C00J-C00Z	1.370(15)	C01R-C01N	1.3900
C00K-C01E	1.434(13)	C02D-C01P	1.3900
C00L-C00R	1.402(14)	C02D-C1	1.3900
C00L-C00T	1.385(13)	C01P-C02M	1.3900
C00M-C01A	1.404(14)	C02M-C01T	1.3900
C00M-C01D	1.374(15)	C01T-C02B	1.3900
C00N-C012	1.403(17)	C02B-C1	1.3900
C00N-C01X	1.39(2)	C19-C424	1.3900
C00O-C00W	1.350(16)	C19-C6	1.3900
C00O-C00Y	1.335(18)	C424-C26	1.3900
C00P-C01C	1.387(16)	C424-C2	1.52(3)
C00R-C00W	1.402(13)	C26-C01Y	1.3900
C00T-C00Y	1.414(15)	C01Y-C01E	1.3900
C00U-C01S	1.3900	C01E-C6	1.3900
C00U-C020	1.3900	O10-C139	1.23(2)
C01S-C02N	1.3900	O14-C139	1.22(2)
C02N-C20	1.3900	O11-C2	1.21(3)
C02N-C139	1.55(2)	C2-O50	1.21(3)
C20-C18	1.3900		

Table S3. Bond Angles for **Cu_3**

Cu03-Cu01-Cu02	60.21(4)	C00Y-C00O-C00W	120.2(9)
P004-Cu01-Cu02	93.55(6)	C00C-C00P-C01C	122.4(10)
P004-Cu01-Cu03	153.68(7)	P008-C00Q-P005	109.8(5)
P005-Cu01-Cu02	152.17(7)	C00W-C00R-C00L	120.5(9)
P005-Cu01-Cu03	93.57(7)	P007-C00S-P004	109.3(4)
P005-Cu01-P004	112.64(8)	C00L-C00T-C00Y	119.9(10)
C00A-Cu01-Cu02	56.3(3)	C01S-C00U-C020	120.0
C00A-Cu01-Cu03	52.2(2)	C00U-C01S-C02N	120.0
C00A-Cu01-P004	113.2(2)	C01S-C02N-C20	120.0
C00A-Cu01-P005	116.6(2)	C01S-C02N-C139	119.0(16)
C00A-Cu01-C017	94.0(4)	C20-C02N-C139	121.0(16)
C017-Cu01-Cu02	52.1(3)	C02N-C20-C18	120.0
C017-Cu01-Cu03	54.7(4)	C020-C18-C20	120.0
C017-Cu01-P004	112.2(4)	C00U-C020-C02E	121.4(9)
C017-Cu01-P005	106.5(3)	C18-C020-C00U	120.0
Cu01-Cu02-Cu03	59.77(4)	C18-C020-C02E	118.6(8)
P006-Cu02-Cu01	150.89(10)	C011-C00V-C00H	117.6(12)
P006-Cu02-Cu03	92.77(8)	C00O-C00W-C00R	120.5(10)
P006-Cu02-P007	111.75(10)	C01W-C00X-C01D	120.9(12)
P007-Cu02-Cu01	96.45(7)	C00O-C00Y-C00T	121.4(10)
P007-Cu02-Cu03	155.27(7)	C018-C00Z-C00J	120.0(9)
C00A-Cu02-Cu01	50.9(2)	C01B-C010-P007	121.9(10)
C00A-Cu02-Cu03	51.0(2)	C01B-C010-C01O	121.0(11)
C00A-Cu02-P006	105.4(2)	C01O-C010-P007	116.4(10)
C00A-Cu02-P007	120.9(2)	C00B-C011-C00V	121.9(10)
C017-Cu02-Cu01	54.6(3)	C00N-C012-P007	122.7(9)
C017-Cu02-Cu03	55.1(4)	C016-C012-P007	120.4(9)
C017-Cu02-P006	119.5(3)	C016-C012-C00N	116.8(11)
C017-Cu02-P007	106.9(4)	C01W-C014-C01A	121.0(10)
C017-Cu02-C00A	91.8(5)	C01U-C015-C016	120.2(13)
Cu01-Cu03-Cu02	60.02(4)	C012-C016-C015	123.3(11)
P008-Cu03-Cu01	97.09(7)	Cu01-C017-Cu03	71.4(4)
P008-Cu03-Cu02	153.78(10)	Cu02-C017-Cu01	73.3(3)
P008-Cu03-P009	108.11(11)	Cu02-C017-Cu03	73.0(3)
P009-Cu03-Cu01	153.49(9)	C02E-C017-Cu01	140.1(8)
P009-Cu03-Cu02	96.77(9)	C02E-C017-Cu02	137.2(13)
C00A-Cu03-Cu01	52.1(2)	C02E-C017-Cu03	133.0(12)
C00A-Cu03-Cu02	56.1(3)	C00Z-C018-C00I	120.3(10)
C00A-Cu03-P008	121.7(3)	P006-C019-P009	108.5(5)
C00A-Cu03-P009	105.6(2)	C014-C01A-C00M	121.6(12)
C00A-Cu03-C017	93.2(4)	C010-C01B-C01Q	121.3(14)
C017-Cu03-Cu01	53.9(2)	C00P-C01C-C01K	116.9(14)
C017-Cu03-Cu02	51.8(3)	C00M-C01D-C00X	119.0(9)

C017-Cu03-P008	105.4(3)	C01H-C01F-C01M	121.1(12)
C017-Cu03-P009	123.5(3)	C01V-C01G-C01M	123.5(18)
C00C-P004-Cu01	116.4(3)	C01F-C01H-C026	118.4(18)
C00C-P004-C00L	103.0(4)	C01Z-C01I-C00C	119.9(13)
C00C-P004-C00S	103.3(4)	C01Z-C01K-C01C	120.7(12)
C00L-P004-Cu01	120.8(3)	C01F-C01M-P008	119.1(9)
C00L-P004-C00S	102.5(4)	C01F-C01M-C01G	116.4(17)
C00S-P004-Cu01	108.8(3)	C01G-C01M-P008	124.5(13)
C00E-P005-Cu01	115.2(3)	C02A-C01O-C010	118.2(17)
C00E-P005-C00J	106.0(4)	C023-C01Q-C01B	116.7(15)
C00E-P005-C00Q	104.8(5)	C015-C01U-C01X	119.4(13)
C00J-P005-Cu01	118.9(3)	C01G-C01V-C026	119.9(15)
C00J-P005-C00Q	100.0(4)	C00X-C01W-C014	119.7(12)
C00Q-P005-Cu01	110.2(3)	C00N-C01X-C01U	118.3(13)
C00M-P006-Cu02	113.5(3)	C01K-C01Z-C01I	119.1(12)
C00M-P006-C01L	100.3(5)	C021-C022-C025	120.0
C019-P006-Cu02	111.8(3)	C022-C021-P009	124.0(6)
C019-P006-C00M	103.3(4)	C022-C021-C02H	120.0
C019-P006-C01L	110.5(5)	C02H-C021-P009	115.9(6)
C01L-P006-Cu02	116.1(3)	C02K-C02H-C021	120.0
C00S-P007-Cu02	110.2(3)	C02H-C02K-C027	120.0
C010-P007-Cu02	115.5(5)	C02K-C027-C025	120.0
C010-P007-C00S	100.2(4)	C027-C025-C022	120.0
C012-P007-Cu02	120.0(4)	C01Q-C023-C02A	124.2(14)
C012-P007-C00S	103.9(5)	C013-C024-C8	120.0
C012-P007-C010	104.6(6)	C01L-C013-C024	120.0
C00Q-P008-Cu03	110.2(4)	C013-C01L-P006	121.6(5)
C00Q-P008-C01M	102.5(5)	C013-C01L-C13	120.0
C01M-P008-Cu03	121.6(4)	C13-C01L-P006	118.3(5)
C01R-P008-Cu03	112.3(4)	C11-C13-C01L	120.0
C01R-P008-C00Q	106.9(5)	C8-C11-C13	120.0
C01R-P008-C01M	102.1(5)	C11-C8-C024	120.0
C019-P009-Cu03	109.5(3)	C01V-C026-C01H	121(2)
C019-P009-C01T	98.4(5)	C01J-C028-C01N	120.0
C021-P009-Cu03	123.0(4)	C02G-C01J-C028	120.0
C021-P009-C019	104.6(5)	C02C-C02G-C01J	120.0
C021-P009-C01T	106.7(5)	C01R-C02C-C02G	120.0
C01T-P009-Cu03	111.7(3)	C02C-C01R-P008	115.9(6)
Cu01-C00A-Cu02	72.8(3)	C02C-C01R-C01N	120.0
Cu03-C00A-Cu01	75.7(3)	C01N-C01R-P008	124.0(6)
Cu03-C00A-Cu02	72.9(3)	C01R-C01N-C028	120.0
C00K-C00A-Cu01	146.8(7)	C01O-C02A-C023	118.2(16)
C00K-C00A-Cu02	128.4(7)	C01P-C02D-C1	120.0
C00K-C00A-Cu03	131.1(7)	C02D-C01P-C02M	120.0

C011-C00B-C00E	119.5(10)	C01T-C02M-C01P	120.0
C00P-C00C-P004	119.5(7)	C02M-C01T-P009	117.7(4)
C00P-C00C-C01I	120.7(10)	C02M-C01T-C02B	120.0
C01I-C00C-P004	119.7(9)	C02B-C01T-P009	121.6(4)
C00F-C00D-C00J	120.9(10)	C1-C02B-C01T	120.0
C00B-C00E-P005	123.6(7)	C02B-C1-C02D	120.0
C00G-C00E-P005	117.5(7)	C017-C02E-C020	170.8(19)
C00G-C00E-C00B	118.8(10)	C424-C19-C6	120.0
C00I-C00F-C00D	119.7(9)	C19-C424-C26	120.0
C00H-C00G-C00E	120.3(9)	C19-C424-C2	126(2)
C00G-C00H-C00V	121.9(10)	C26-C424-C2	114(2)
C00F-C00I-C018	120.4(9)	C01Y-C26-C424	120.0
C00D-C00J-P005	124.5(8)	C01E-C01Y-C26	120.0
C00Z-C00J-P005	116.9(6)	C01Y-C01E-C00K	121.1(7)
C00Z-C00J-C00D	118.4(8)	C01Y-C01E-C6	120.0
C00A-C00K-C01E	178.8(11)	C6-C01E-C00K	117.8(7)
C00R-C00L-P004	123.8(6)	C01E-C6-C19	120.0
C00T-C00L-P004	118.8(7)	O11-C2-C424	125(5)
C00T-C00L-C00R	117.3(8)	O11-C2-O50	127(5)
C01A-C00M-P006	119.9(9)	O50-C2-C424	107(4)
C01D-C00M-P006	122.0(7)	O10-C139-C02N	114(3)
C01D-C00M-C01A	117.7(10)	O10-C139-O14	126(3)
C01X-C00N-C012	121.8(13)	O14-C139-C02N	120(3)

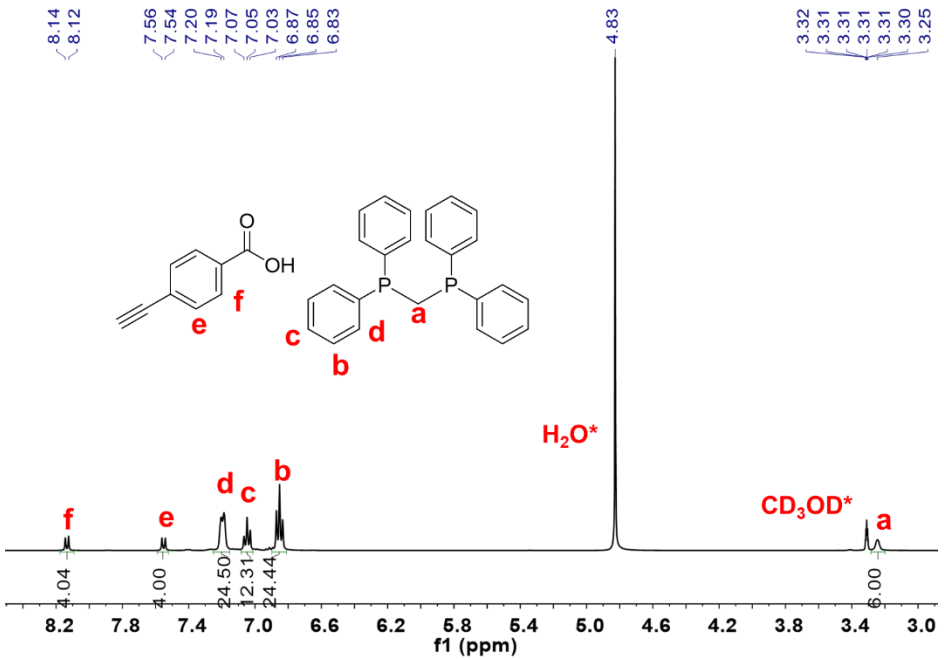

Fig. S1. ^{1}H NMR spectrum of **Cu$_3$** (400 MHz, CD_3OD, 298 K).

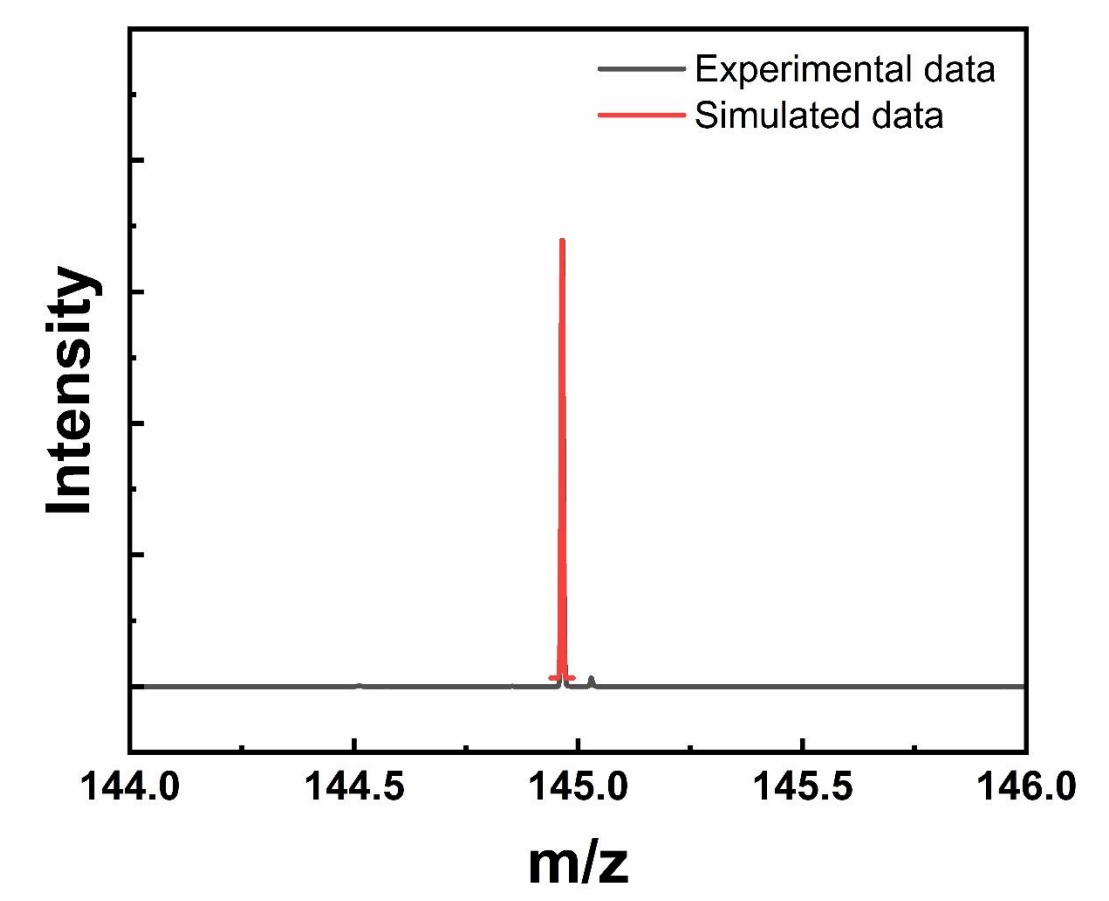

Fig. S2. Negative mode ESI-MS spectrum of **Cu$_3$** in MeOH.

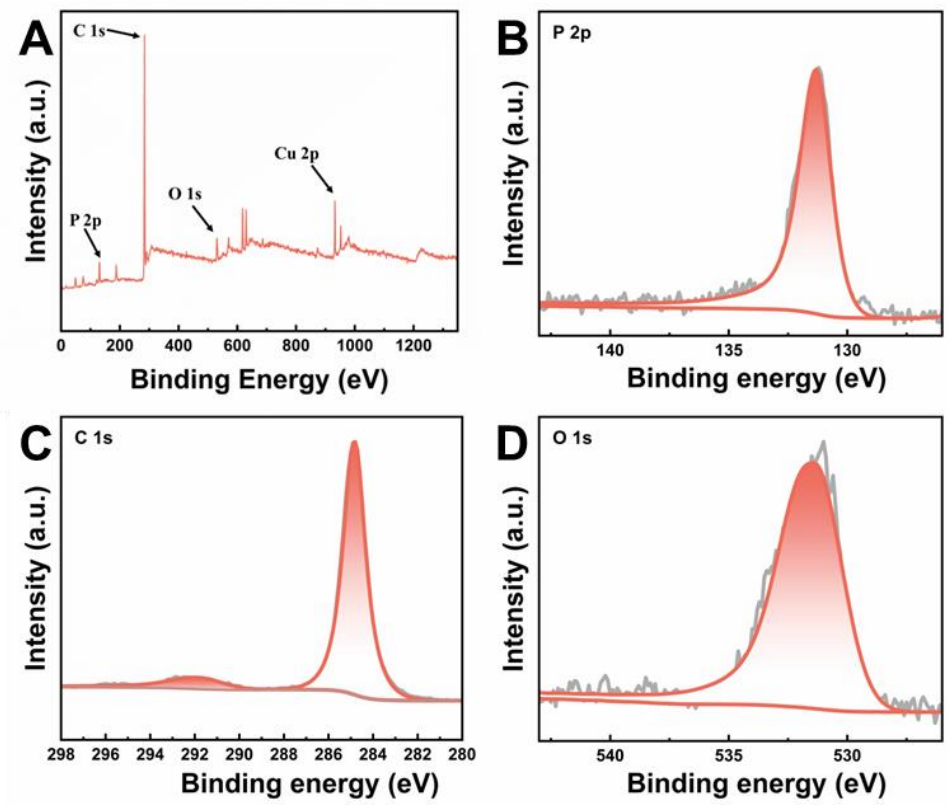

Fig. S3. XPS spectra of **Cu_3** : Full scan(A), P 2p(B), C 1s(C), and O 1s(D).

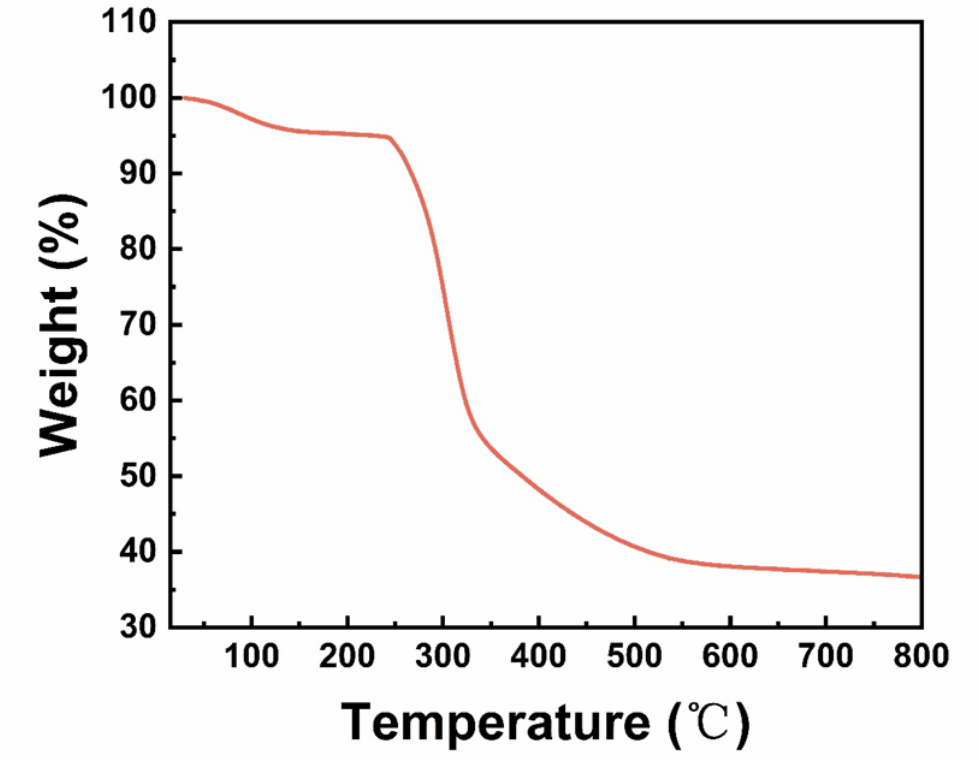

Fig. S4. TGA plot of **Cu_3** nanocluster.

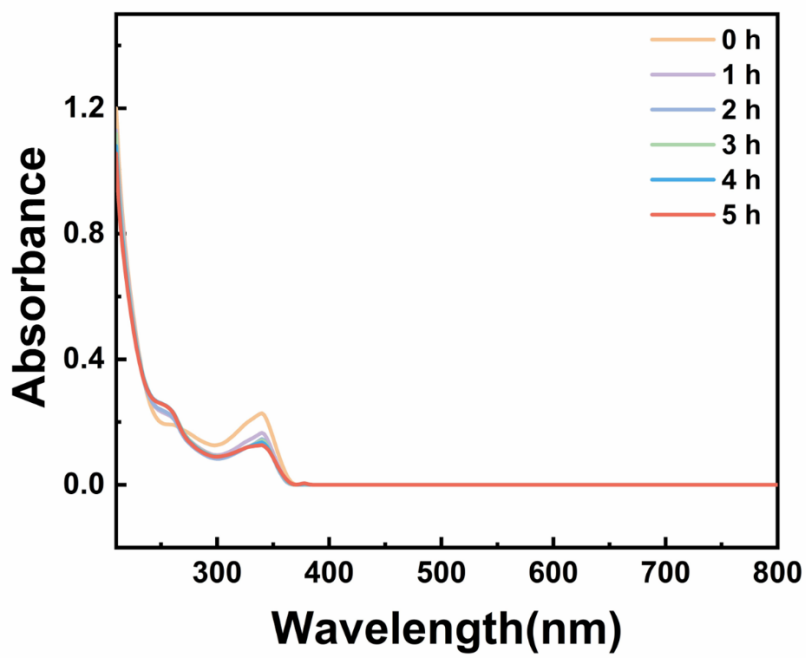

Fig. S5. UV monitoring curve of **Cu$_3$** nanocluster.

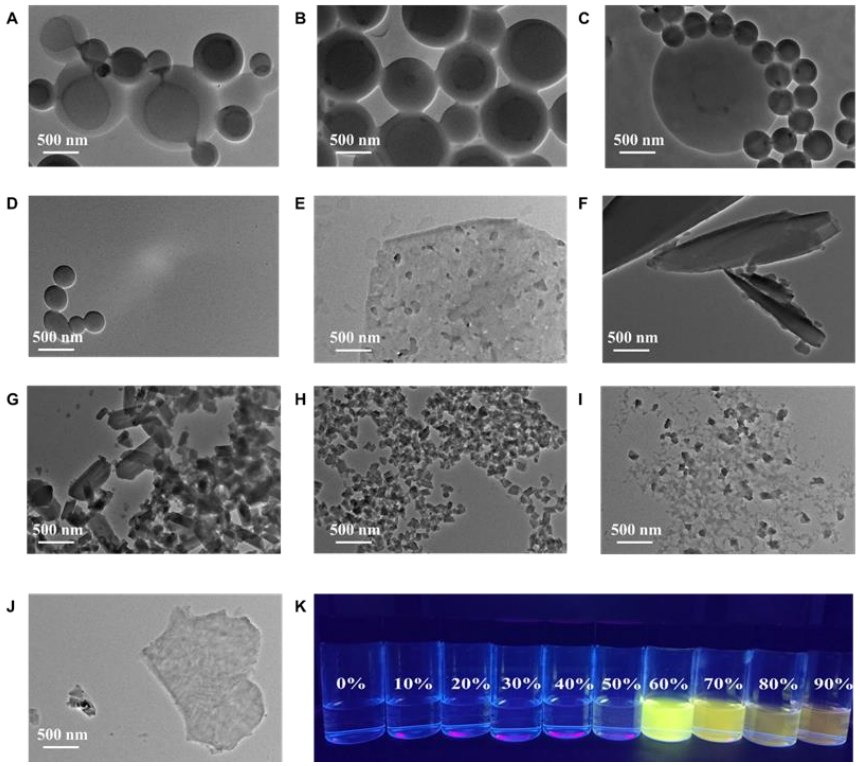

Fig. S6. TEM image of **Cu$_3$** in H_2O/MeOH mixtures with different f_{water} values(500nm). (A): f_{water}=0%; (B): f_{water}=10%; (C): f_{water}=20%; (D): f_{water}=30%; (E): f_{water}=40%; (F): f_{water}=50%; (G): f_{water}=60%; (H): f_{water}=70%; (I): f_{water}=80%; (J): f_{water}=90%; (K): The higher the volume fraction of **Cu$_3$** in the solution, the greater the discharge intensity in the photograph.

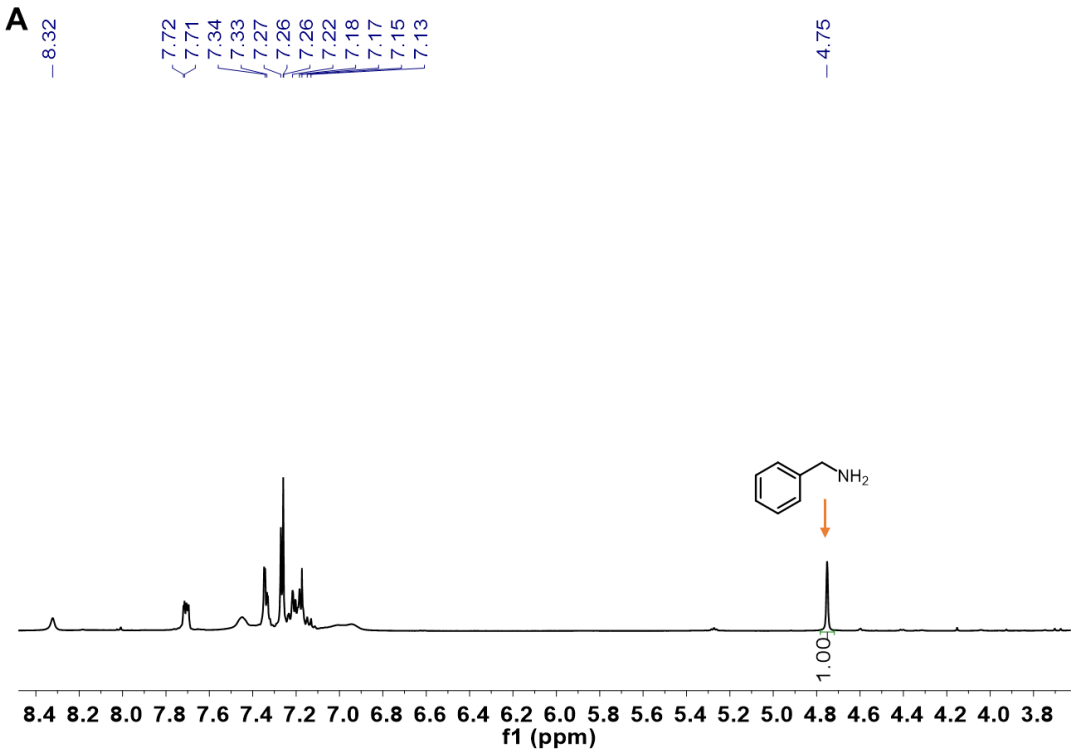
A
8.32
7.72
7.71
7.34
7.33
7.27
7.26
7.26
7.22
7.18
7.17
7.15
7.13
4.75
NH2
1.00
8.4 8.2 8.0 7.8 7.6 7.4 7.2 7.0 6.8 6.6 6.4 6.2 6.0 5.8 5.6 5.4 5.2 5.0 4.8 4.6 4.4 4.2 4.0 3.8
f1 (ppm)

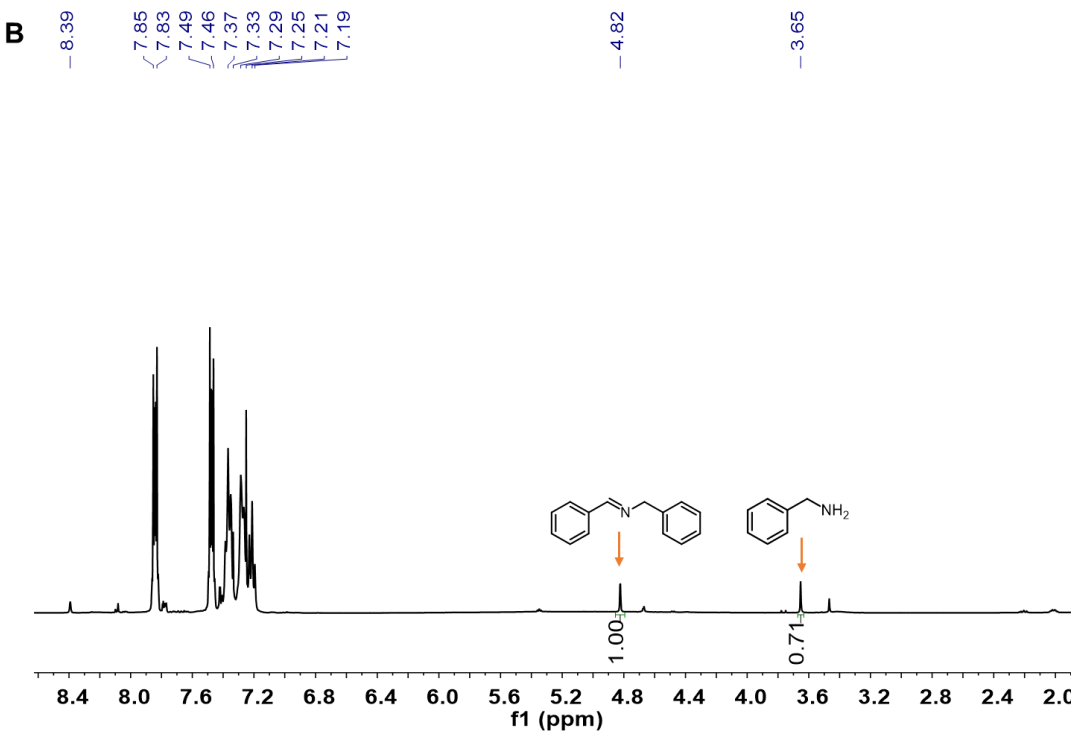
B
8.39
7.85
7.83
7.49
7.46
7.37
7.33
7.29
7.25
7.21
7.19
4.82
3.65
N
NH2
1.00
0.71
8.4 8.0 7.6 7.2 6.8 6.4 6.0 5.6 5.2 4.8 4.4 4.0 3.6 3.2 2.8 2.4 2.0
f1 (ppm)

C

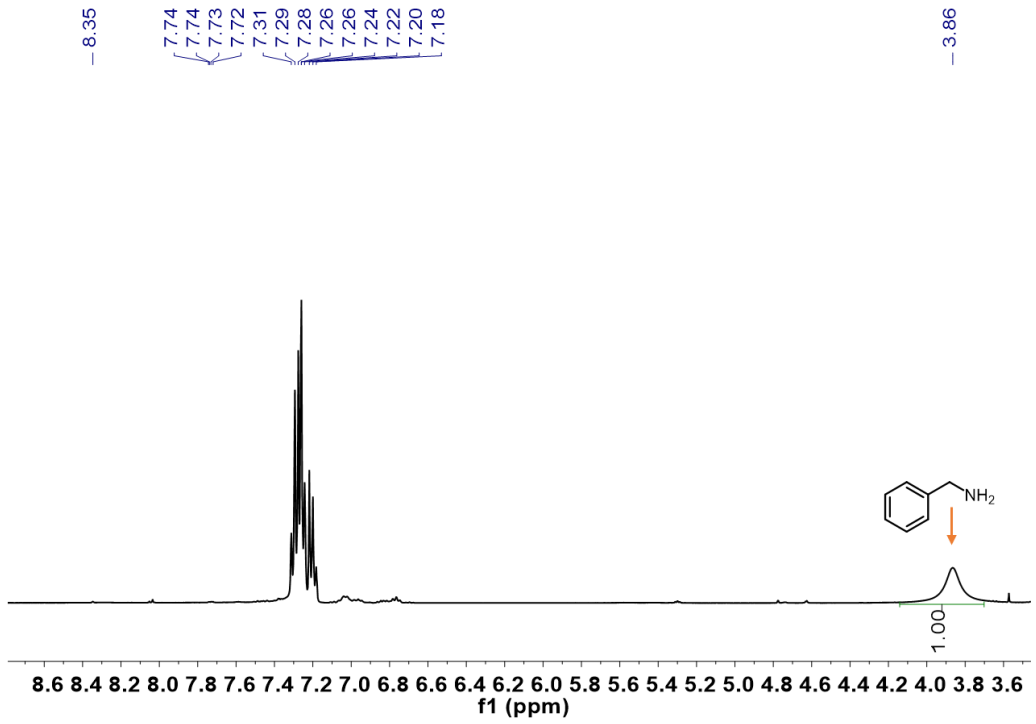
8.35
7.74
7.74
7.73
7.72
7.31
7.29
7.28
7.26
7.26
7.24
7.22
7.20
7.18
3.86
NH2
1.00
8.6 8.4 8.2 8.0 7.8 7.6 7.4 7.2 7.0 6.8 6.6 6.4 6.2 6.0 5.8 5.6 5.4 5.2 5.0 4.8 4.6 4.4 4.2 4.0 3.8 3.6
f1 (ppm)

D

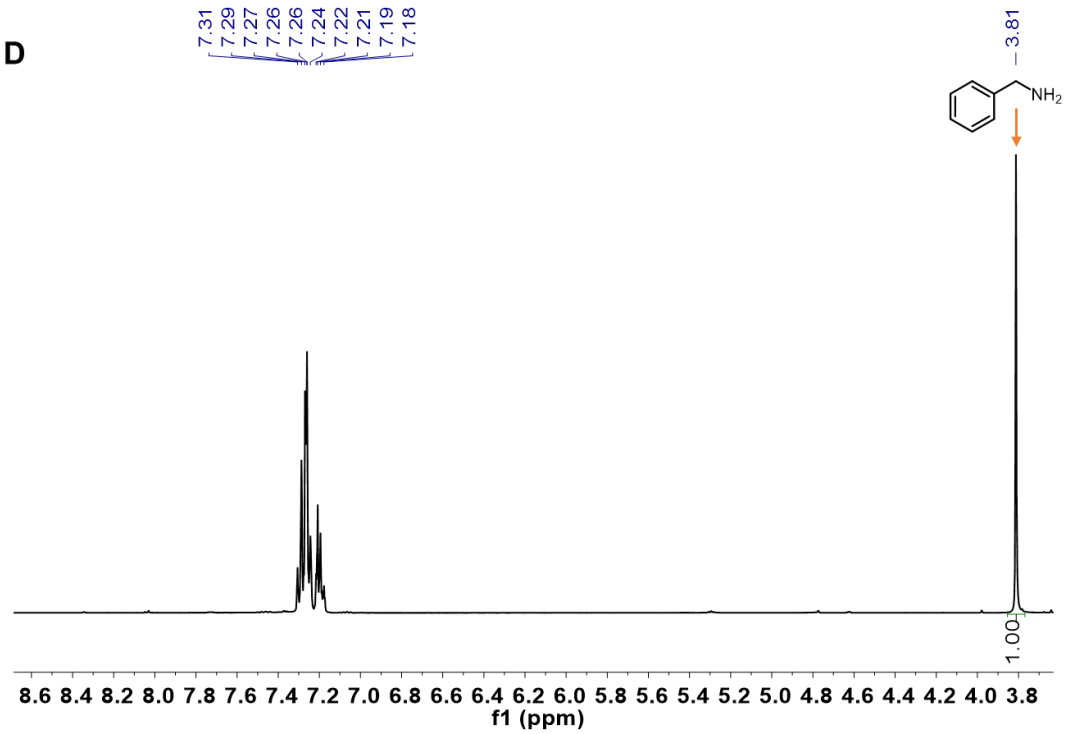
7.31
7.29
7.27
7.26
7.26
7.24
7.22
7.21
7.19
7.18
3.81
NH2
1.00
8.6 8.4 8.2 8.0 7.8 7.6 7.4 7.2 7.0 6.8 6.6 6.4 6.2 6.0 5.8 5.6 5.4 5.2 5.0 4.8 4.6 4.4 4.2 4.0 3.8
f1 (ppm)

E

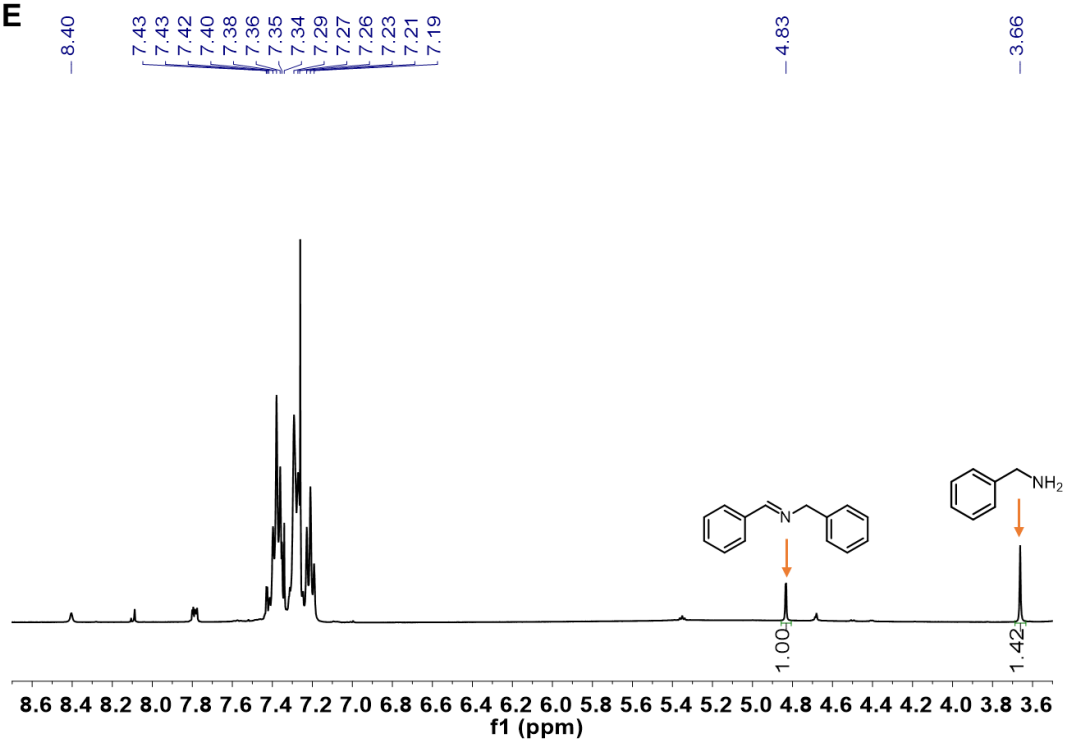
8.40
7.43
7.43
7.42
7.40
7.38
7.36
7.35
7.34
7.29
7.27
7.26
7.23
7.21
7.19
4.83
3.66
NH2
N
1.00
1.42
8.6 8.4 8.2 8.0 7.8 7.6 7.4 7.2 7.0 6.8 6.6 6.4 6.2 6.0 5.8 5.6 5.4 5.2 5.0 4.8 4.6 4.4 4.2 4.0 3.8 3.6
f1 (ppm)

F

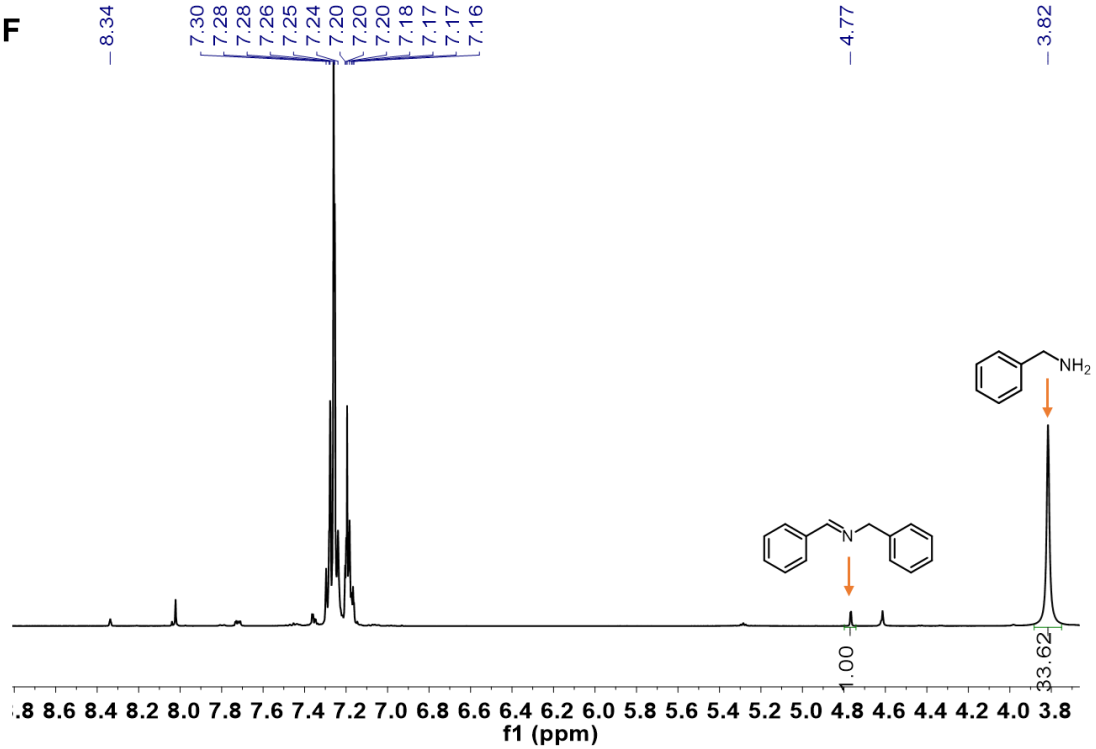
8.34
7.30
7.28
7.28
7.26
7.25
7.24
7.20
7.20
7.20
7.18
7.17
7.17
7.16
4.77
3.82
NH2
N
1.00
33.62
8.6 8.4 8.2 8.0 7.8 7.6 7.4 7.2 7.0 6.8 6.6 6.4 6.2 6.0 5.8 5.6 5.4 5.2 5.0 4.8 4.6 4.4 4.2 4.0 3.8
f1 (ppm)

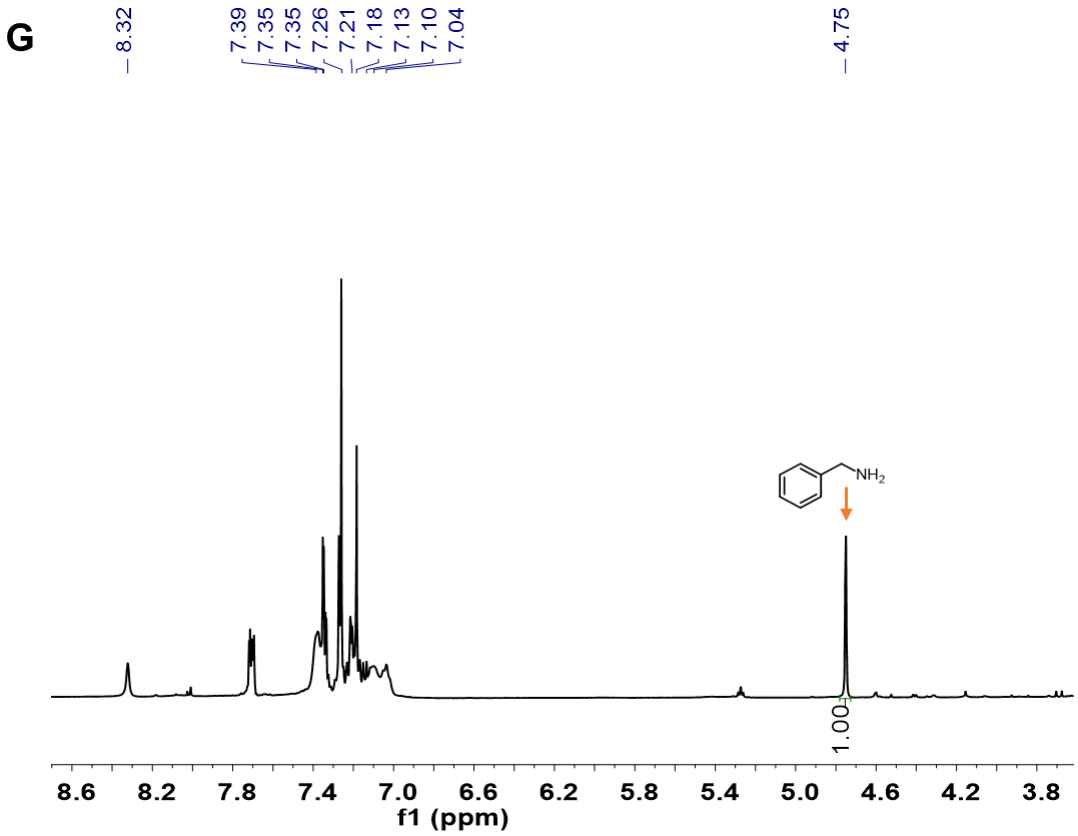

Fig. S7. ^{1}H NMR signals of benzylamine. (A): Table 1, entry 1; (B): Table 1, entry 2; (C): Table 1, entry 3; (D): Table 1, entry 4; (E): Table 1, entry 5; (F): Table 1, entry 6; (G): Table 1, entry 7.

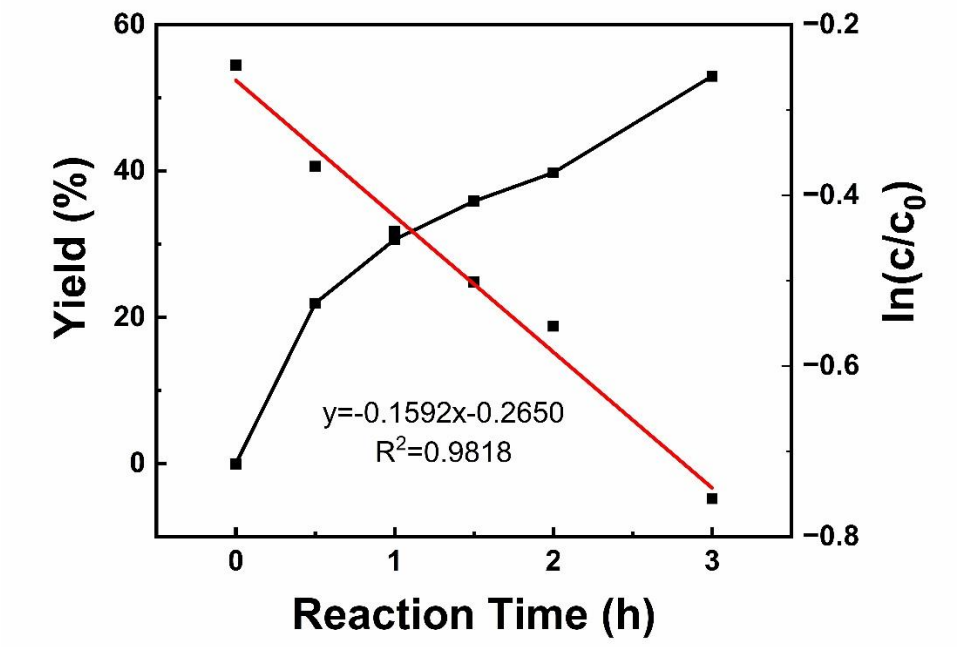

Fig. S8. Kinetic study of the oxidative coupling of benzylamine catalyzed by **Cu3**.

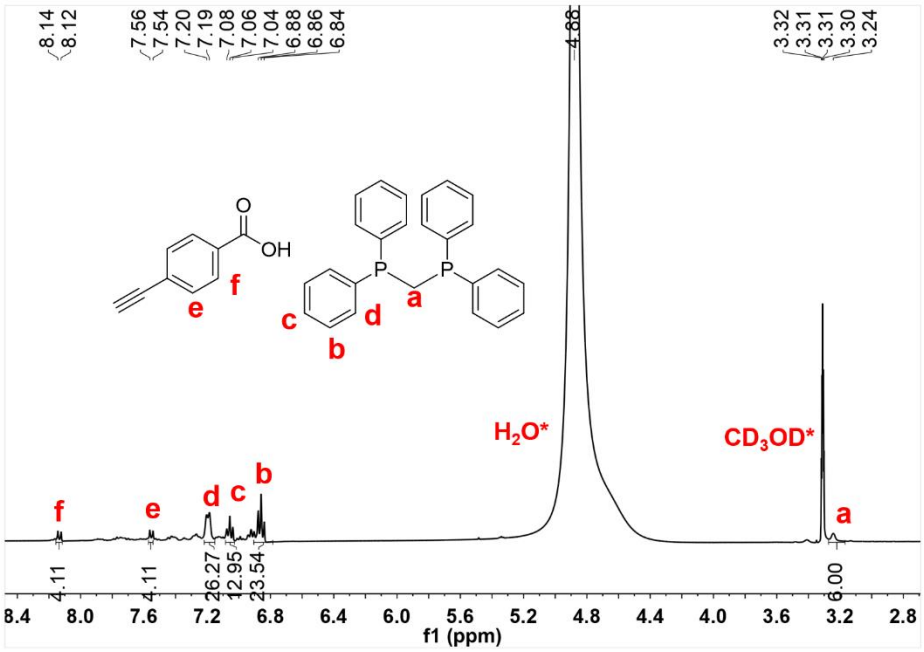

Fig. S9. ^{1}H NMR spectrum of **Cu$_3$** after catalytic reaction. (400 MHz, CD_3OD, 298 K).

Table S4. Experiments on the Expansion of Photocatalytic Benzylamine Coupling Substrates

Entry	Substrate	Product	Conversion(%)
1	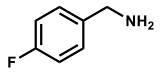	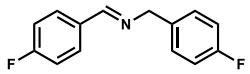	99
2	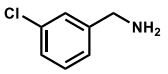	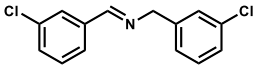	99
3	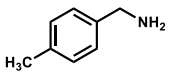	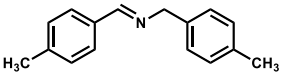	99
4	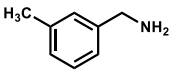	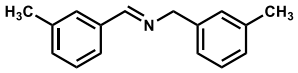	99
5	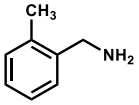	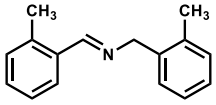	99
6	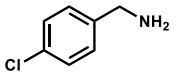	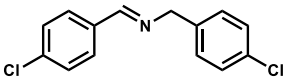	88

A

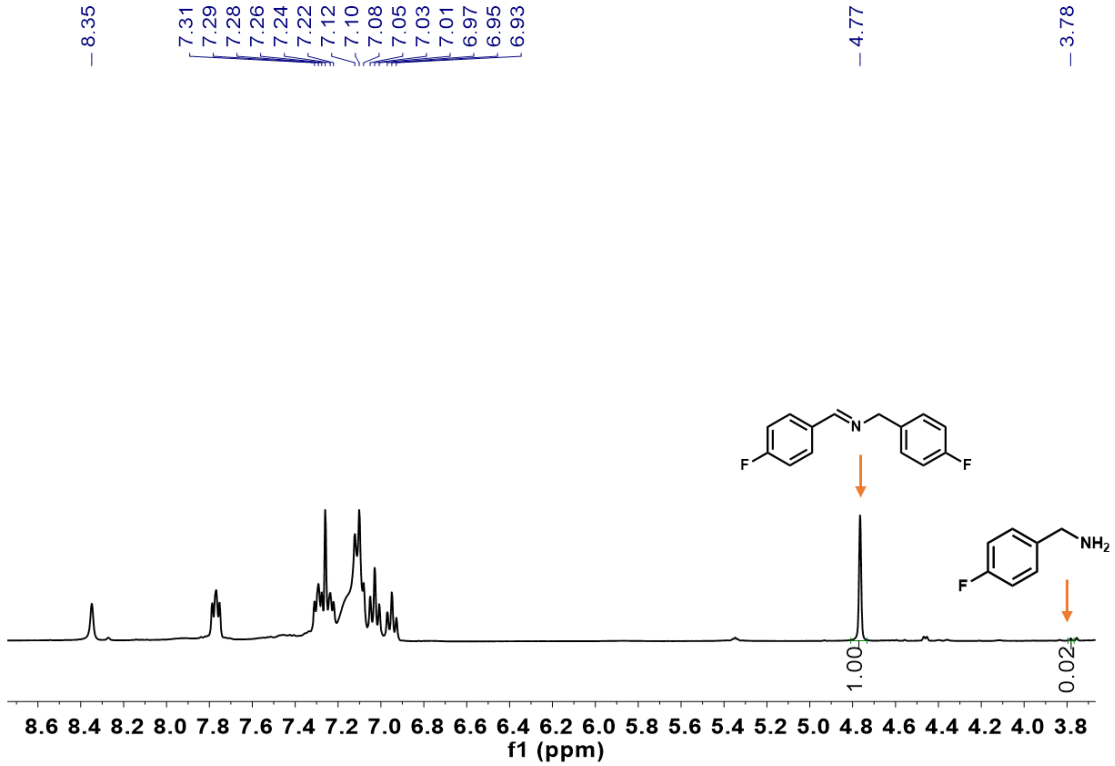
8.35
7.31
7.29
7.28
7.26
7.24
7.22
7.12
7.10
7.08
7.05
7.03
7.01
6.97
6.95
6.93
4.77
3.78
F
N
F
NH2
F
1.00
0.02
8.6 8.4 8.2 8.0 7.8 7.6 7.4 7.2 7.0 6.8 6.6 6.4 6.2 6.0 5.8 5.6 5.4 5.2 5.0 4.8 4.6 4.4 4.2 4.0 3.8
f1 (ppm)

B

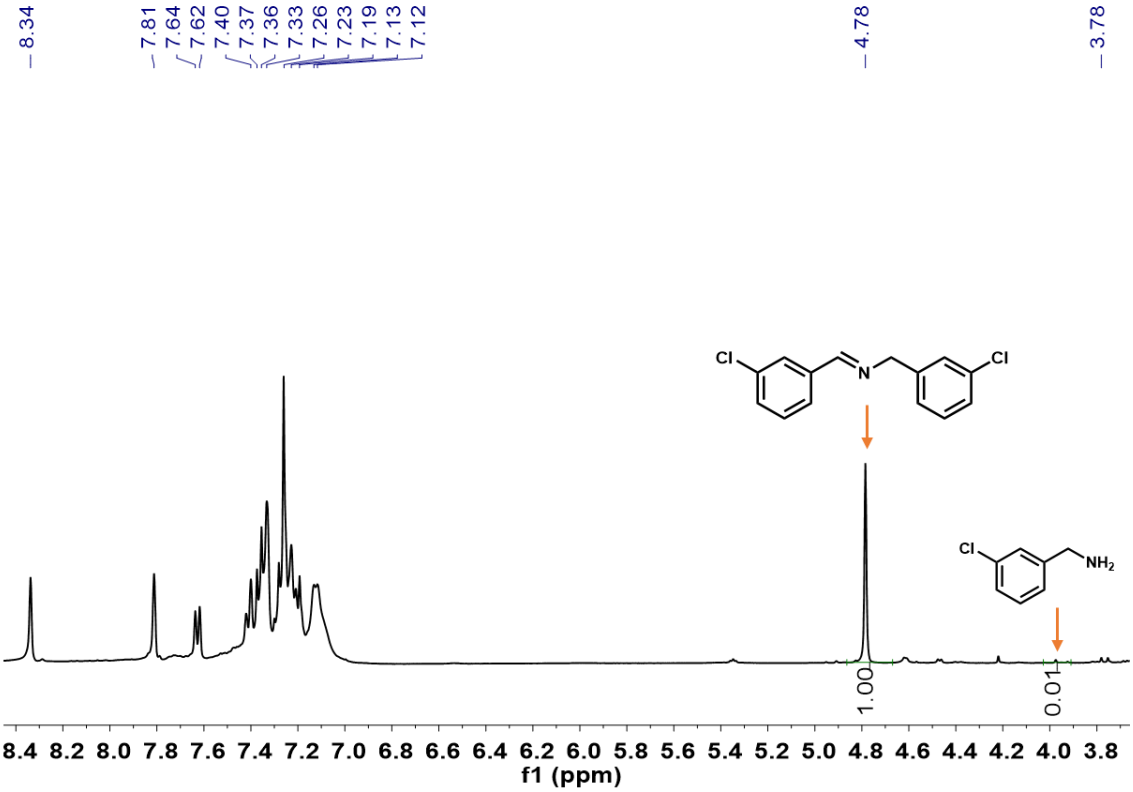
8.34
7.81
7.64
7.62
7.40
7.37
7.36
7.33
7.26
7.23
7.19
7.13
7.12
4.78
3.78
Cl
N
Cl
Cl
NH2
1.00
0.01
8.4 8.2 8.0 7.8 7.6 7.4 7.2 7.0 6.8 6.6 6.4 6.2 6.0 5.8 5.6 5.4 5.2 5.0 4.8 4.6 4.4 4.2 4.0 3.8
f1 (ppm)

C

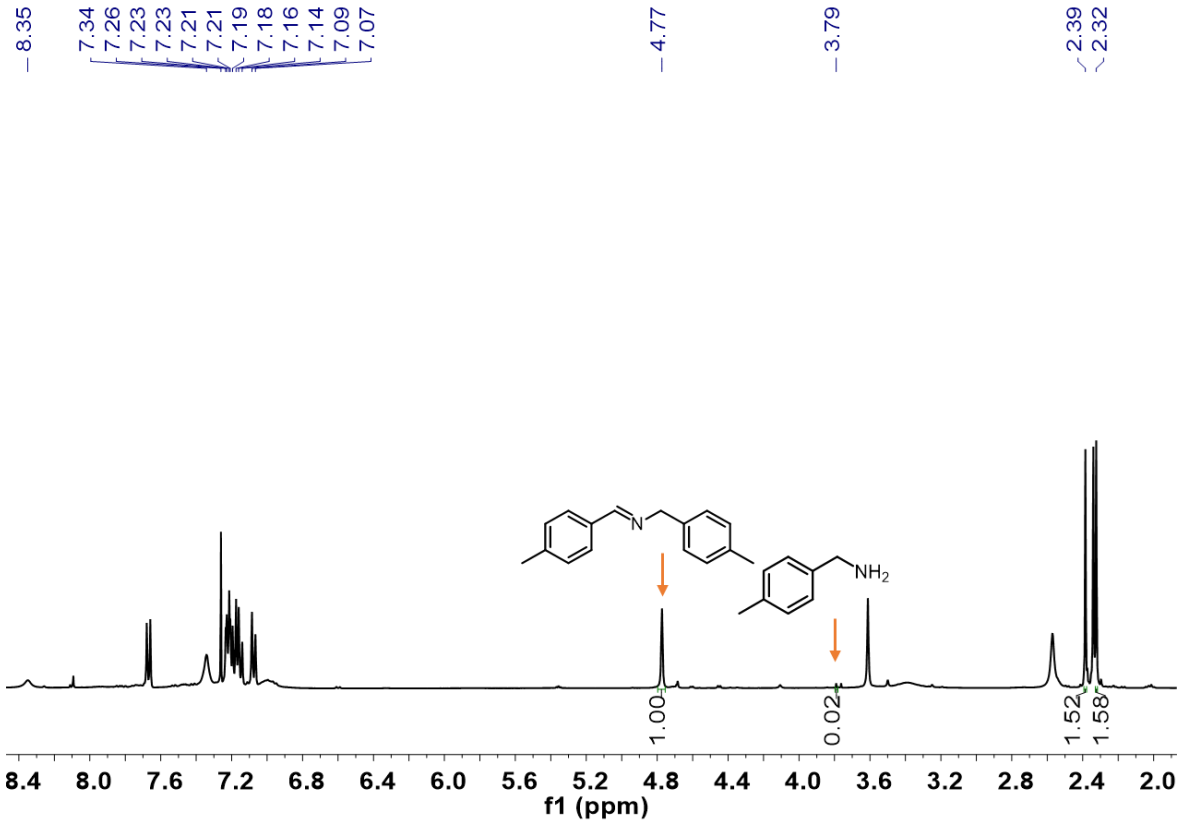
8.35
7.34
7.26
7.23
7.23
7.21
7.21
7.19
7.18
7.16
7.14
7.09
7.07
4.77
3.79
2.39
2.32
NH2
1.00
0.02
1.52
1.58
8.4 8.0 7.6 7.2 6.8 6.4 6.0 5.6 5.2 4.8 4.4 4.0 3.6 3.2 2.8 2.4 2.0
f1 (ppm)

D

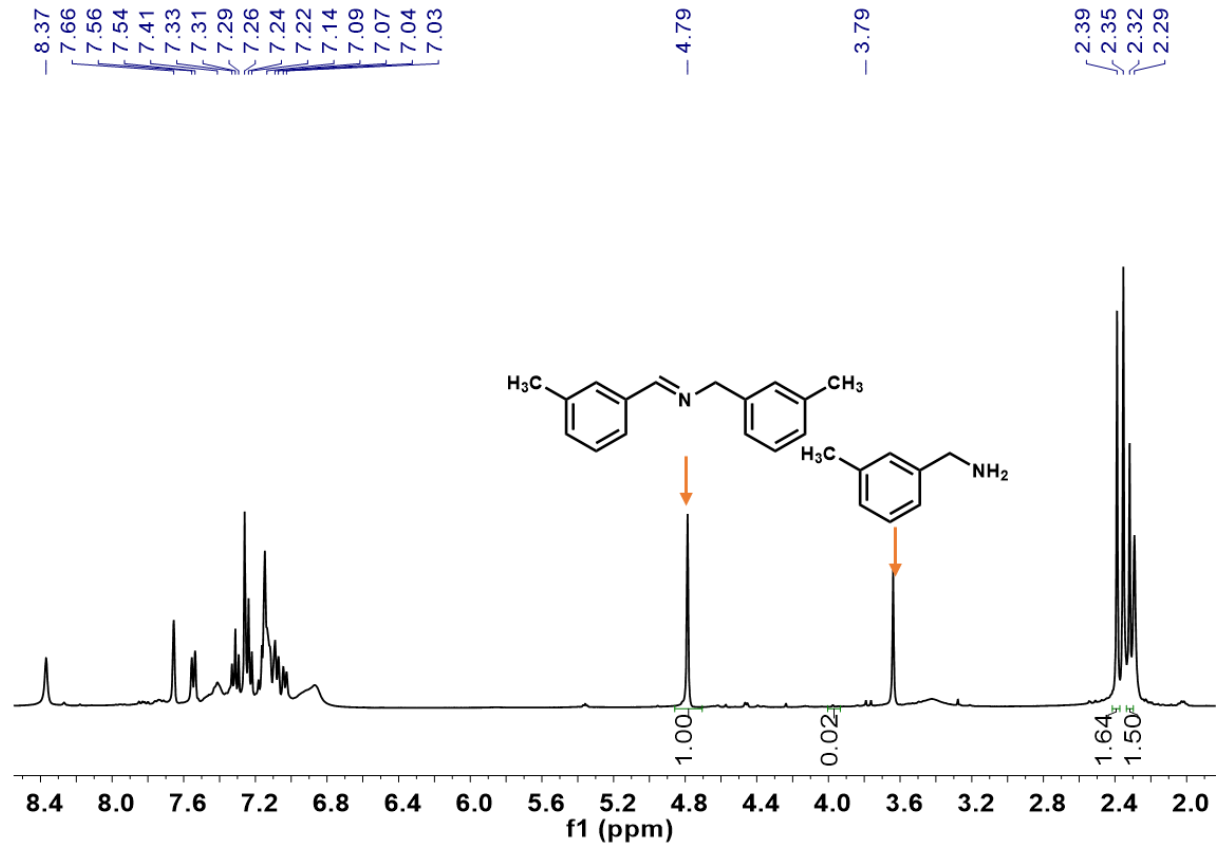
8.37
7.66
7.56
7.54
7.41
7.33
7.31
7.29
7.26
7.24
7.22
7.14
7.09
7.07
7.04
7.03
4.79
3.79
2.39
2.35
2.32
2.29
H3C
CH3
H3C
NH2
1.00
0.02
1.64
1.50
8.4 8.0 7.6 7.2 6.8 6.4 6.0 5.6 5.2 4.8 4.4 4.0 3.6 3.2 2.8 2.4 2.0
f1 (ppm)

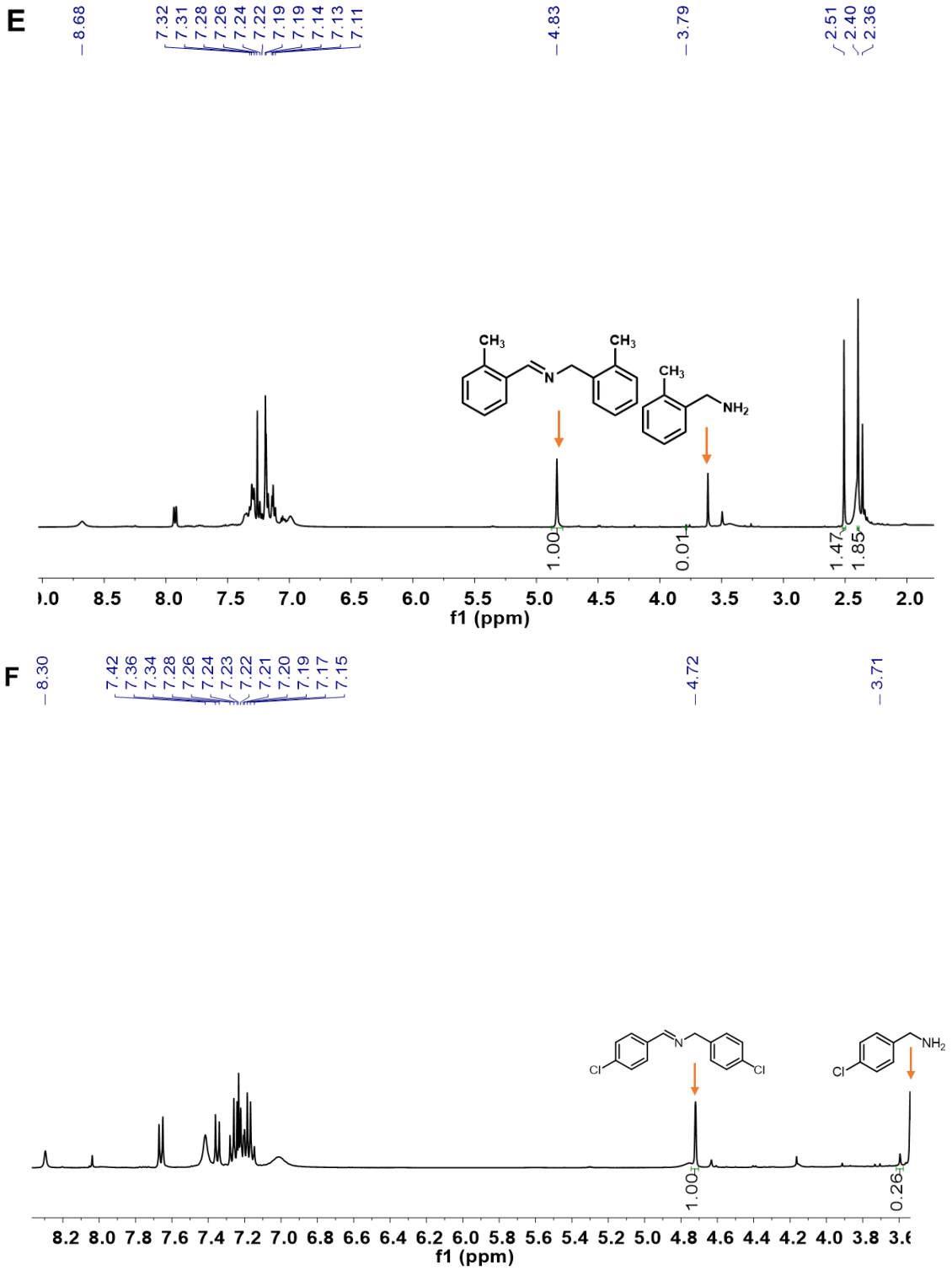

Fig. S10. ^{1}H NMR signals of phenethylamine derivatives. (A): Table S4, entry 1; (B): Table S4, entry 2; (C): Table S4, entry 3; (D): Table S4, entry 4; (E): Table S4, entry 5; (F): Table S4, entry 6.